Ground State of Graphene in the Presence of Random Charged Impurities

Enrico Rossi and S. Das Sarma

Condensed Matter Theory Center, Department of Physics, University of Maryland, College Park, Maryland 20742, USA

(Received 17 March 2008; published 15 October 2008)

We calculate the carrier-density-dependent ground-state properties of graphene in the presence of random charged impurities in the substrate taking into account disorder and interaction effects nonperturbatively on an equal footing in a self-consistent theoretical formalism. We provide detailed quantitative results on the dependence of the disorder-induced spatially inhomogeneous two-dimensional carrier density distribution on the external gate bias, the impurity density, and the impurity location. We find that the interplay between disorder and interaction is strong, particularly at lower impurity densities. We show that, for the currently available typical graphene samples, inhomogeneity dominates graphene physics at low ($\lesssim 10^{12}$ cm^{-2}) carrier density with the density fluctuations becoming larger than the average density.

DOI: 10.1103/PhysRevLett.101.166803 PACS numbers: 73.21.−b, 71.20.Tx, 81.05.Uw

The recent experimental realization [1] of single-layer graphene sheets has spurred an enormous amount of activity in studying the electronic properties of 2D chiral Dirac fermions in the context of solid state materials physics. While much of this interest is fundamental, a substantial part of it also derives from the technological prospect of graphene being used as a novel transistor material. To understand current experiments and be able to design future graphene-based electronic devices, it is essential to know the properties, origin, and effects of extrinsic disorder in graphene. The low energy electronic states of graphene are described by a massless Dirac equation. In clean isolated graphene (the so-called intrinsic graphene), the Fermi energy lies exactly at the Dirac point (i.e., the charge neutrality point) where the linear chiral electron and hole bands cross each other. Several works [2] calculated the graphene conductivity assuming the graphene Fermi energy to be exactly at the Dirac point throughout the graphene layer. These works found the Dirac point conductivity to be either 0, ∞, or, in the limit of vanishing disorder, equal to the universal value $\sigma_D \equiv 4e^2/\pi\hbar$. In current experiments, however, the measured conductivity at the Dirac point [3] is finite and much bigger (by a factor of 2–20) than σ_D and varies strongly from sample to sample. The discrepancy can be resolved if we consider that disorder in addition to representing the main source of scattering has another important effect: It locally shifts the Dirac point removing, at zero gate voltage, the Fermi energy from the charge neutrality point [4]. This leads immediately to a disorder-induced inhomogeneous density landscape with electron-hole puddles. Such puddles have been proposed theoretically [5] and observed experimentally [6,7]. Experiments, by themselves, are unable to directly identify the cause of the carrier density inhomogeneities. Two kinds of disorder have been proposed in graphene to have this effect: ripples [8] and random charge impurities [5]. Transport theories [5,9–11] based on the presence of charge impurities have been successful in explaining the experimental results [3]. But whether the puddles arise from the random charged impurities or from some other mechanism [8] has remained an open question. We provide in this Letter the first realistic theoretical description of the electron-hole puddles in graphene assuming the random charged impurity disorder to be the underlying mechanism. Our theoretical results are in excellent qualitative agreement with the existing experimental data [6,7]. A quantitative comparison between our results and future experiments with higher quantitative accuracy would enable a definitive understanding of the nature of the disorder in graphene.

At low energies the quasiparticles in graphene can be described by a massless Dirac-fermion (MDF) model with an ultraviolet cutoff wave vector k_c. We set $k_c = 1/a_0$, where a_0 is the graphene lattice constant, $a_0 = 0.246$ nm, corresponding to an energy cutoff $E_c \approx 3$ eV, and measure the energies from the Dirac point. To find the ground-state carrier density n, we use the Thomas-Fermi-Dirac (TF) theory. In contrast with the standard TF theory, we retain the exchange potential nonperturbatively through its local density approximation so that the energy functional $E[n]$ reads

$$E[n] = \hbar v_F \Big[\frac{2\sqrt{\pi}}{3} \int d^2 r \,\mathrm{sgn}(n) |n|^{3/2} + \frac{r_s}{2} \int d^2 r \int d^2 r' \frac{n(\mathbf{r}) n(\mathbf{r}')}{|\mathbf{r} - \mathbf{r}'|} + \frac{E_{xc}[n]}{\hbar v_F} + r_s \int d^2 r V_D(\mathbf{r}) n(\mathbf{r}) - \frac{\mu}{\hbar v_F} \int d^2 r n(\mathbf{r}) \Big], \quad (1)$$

where $v_F = 10^6$ m/s is the Fermi velocity, $r_s \equiv e^2/(\hbar v_F \epsilon)$ is the coupling constant with ϵ the effective background dielectric constant, $E_{xc}[n]$ is the exchange energy, V_D is the disorder potential, and μ is the chemical potential. The first two terms in (1) are the kinetic energy and the Hartree part of the Coulomb interaction, respectively. For graphene on a SiO_2 substrate, $\epsilon = 2.5$ and then $r_s = 0.8$. By differentiating $E[n]$ with respect to n, we find

$$\frac{\delta E}{\delta n} = \hbar v_F \left[\mathrm{sgn}(n)\sqrt{\pi|n|} + \frac{r_s}{2} \int \frac{n(\mathbf{r}')d^2r'}{|\mathbf{r}-\mathbf{r}'|} + r_s V_D \right] + \Sigma(n) - \mu, \quad (2)$$

where $\Sigma(n)$ is the Hartree-Fock self-energy [12,13] evaluated at the Fermi wave vector $k_F = \mathrm{sgn}(n)\sqrt{\pi|n|}$:

$$\frac{\Sigma(n)}{\hbar v_F} = \sqrt{\pi|n|}\,\mathrm{sgn}(n) r_s \left[\frac{1}{4} \ln \frac{4k_c}{\sqrt{\pi|n|}} - \left(\frac{2C+1}{2\pi} + \frac{1}{8} \right) \right], \quad (3)$$

where $C \approx 0.916$.

We assume V_D to be the 2D Coulomb potential in the graphene plane generated by a random 2D distribution $C(\mathbf{r})$ of impurity charges placed at a distance d from the graphene layer. Denoting by angular brackets the average over disorder realizations, we assume

$$\langle C(\mathbf{r}) \rangle = 0, \qquad \langle C(\mathbf{r}_1) C(\mathbf{r}_2) \rangle = n_{\mathrm{imp}} \delta(\mathbf{r}_2 - \mathbf{r}_1), \quad (4)$$

where n_{imp} is the 2D impurity density. A nonzero value of $\langle C(\mathbf{r}) \rangle$ can be taken into account by a shift of μ, i.e., of the gate voltage. n_{imp} and d should be taken as effective parameters characterizing the impurity distribution in a minimal two-parameter model. In current graphene samples obtained through mechanical exfoliation, possible sources of charge impurities are most likely ions in the substrate that drift close to the surface, charges trapped between the graphene layer and the substrate, and free charges that stick to the top surface of the graphene layer. This picture is consistent with the vast literature on disorder in Si metal-oxide-semiconductor field-effect transistors (MOSFETs) and has recently been indirectly confirmed by experiments on suspended graphene [14]. The values of n_{imp} extracted from transport measurements, and used in this work, are indeed of the same order of magnitude $[10^{11}$–$10^{12}]$ cm^{-2} as the ones used to describe quantitatively disorder effects of MOSFET devices on SiO_2. Combining Eqs. (2)–(4), we find the ground-state carrier density by solving the equation $\delta E/\delta n = 0$ using the steepest descent method. Our calculations are done for a finite square lattice of size $L \times L$. All of the results presented in this Letter are obtained for $L = 200$ nm and are found to be independent of system size for $L \gtrsim 100$ nm. For the discretization in real space, we use a 1 nm step.

For a given disorder realization, for $\mu = 0$, a typical result, including exchange, for $n(\mathbf{r})$ is shown in Fig. 1(a). For $n > 0$ ($n < 0$), we have particles (holes). The result without exchange is characterized by larger density fluctuations. This is clear from Fig. 1(b), which shows that the density distribution is more strongly peaked around $n = 0$ when exchange is taken into account. The result of Fig. 1(b) is counterintuitive because exchange suppresses density inhomogeneity instead of enhancing it as in parabolic-band inhomogeneous electron liquids. A complementary density-functional theory local-density approximation (DFT-LDA) calculation, using single disorder realizations with few impurities, has also found similar results [15]. Contrary to our work in Ref. [15], the correlation contributions have been taken into account. Given the numerical complexity of the DFT-LDA approach, in Ref. [15] only small samples were considered and disorder-averaged results, that would permit a close quantitative comparison, were not presented. The results for single disorder realizations are qualitatively similar to ours, showing that correlation terms have only a minor quantitative effect. The reason is that in graphene to very good approximation the correlation term scales with n in the same way as exchange [12,15] but with opposite sign, and therefore its effect is to simply reduce the exchange strength.

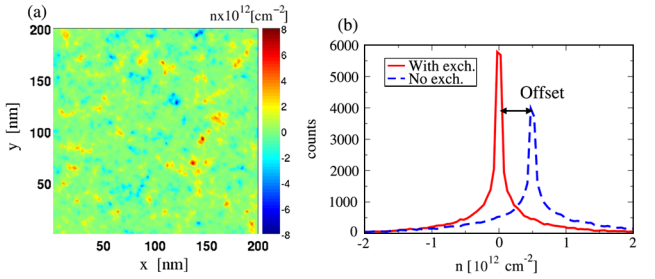

FIG. 1 (color online). Results at the Dirac point for a disorder realization assuming $n_{\mathrm{imp}} = 10^{12}$ cm^{-2}, $d = 1$ nm, and $\epsilon = 2.5$. (a) Color plot of $n(\mathbf{r})$ including exchange. (b) Density distribution for $n(\mathbf{r})$ shown in (a). For clarity, the result without exchange has been offset along the x axis.

The results of Fig. 1 are visually very similar to the ones observed in experiments [6,7], but a quantitative comparison can be achieved only by calculating the disorder-averaged statistical properties. For a given quantity X, we therefore calculate its disorder-averaged value $\langle X \rangle$ and spatial correlation function $\langle [\delta X(\mathbf{r})]^2 \rangle = \langle [X(\mathbf{r}) - \langle X \rangle] \times [X(0) - \langle X \rangle] \rangle$. From these results, we extract the rms of the fluctuations $X_{\mathrm{rms}} \equiv \sqrt{\langle [\delta X(0)]^2 \rangle}$ and their typical correlation length $\xi_X \equiv$ FWHM of $\langle [\delta X(\mathbf{r})]^2 \rangle$. At the neutrality point, $\xi \equiv \xi_n$ can be loosely taken as a measure of the electron-hole puddle size. In Fig. 2, we present the disordered averaged results at the Dirac point as a function of n_{imp}. We see that exchange suppresses the amplitude of the density fluctuations and increases their correlation length and that its effect becomes increasingly important as the impurity density decreases; for the lowest n_{imp}, the value of n_{rms} including exchange is 3 times smaller than the value obtained without exchange [Fig. 2(a)]. In addition, we see that the scaling of n_{rms} with n_{imp} is very different with and without exchange. From Fig. 2(b), we see that as n_{imp} decreases ξ increases very slowly, especially for low values of d, a result that underlines the importance of nonlinear screening terms. Adapted to a 2D distribution of charges, the approach used in Ref. [16] for the scaling of ξ on n_{imp} gives $\xi \approx 1/(r_s^2\sqrt{n_{\mathrm{imp}}})$. For $r_s = 0.8$ and

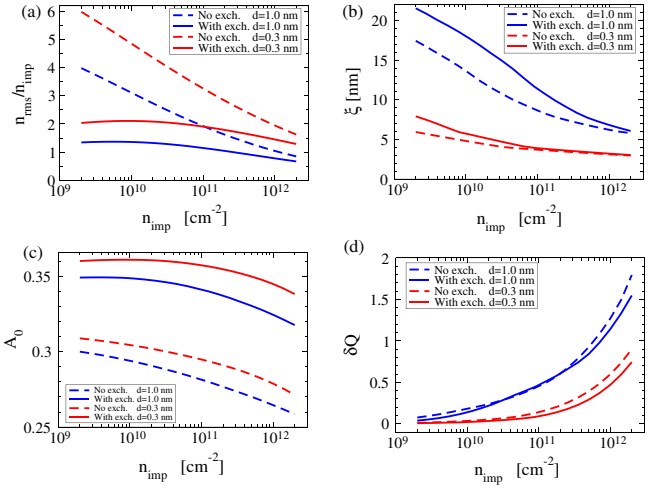

FIG. 2 (color online). Results as a function of $n_{\rm imp}$ at the Dirac point for $d = 1$ nm (blue lines) and $d = 0.3$ nm (red lines). $\epsilon = 2.5$. (a) $n_{\rm rms}$; (b) ξ; (c) A_0; (d) δQ.

$n_{\rm imp} = 2 \times 10^9$ cm^{-2}, we would then expect $\xi \approx 350$ nm, a value an order of magnitude larger than the value shown in Fig. 2(b). The reason for this discrepancy is that for small values of $n_{\rm imp}$ the carrier distribution is not characterized by smooth long-range fluctuations but rather by wide regions of very small carrier density (≈ 0) interspersed with small electron-hole puddles with the typical size ξ shown in Fig. 2(b). This picture is confirmed in Fig. 2(c) where the disorder-averaged area fraction A_0, over which $|n(\mathbf{r}) - \langle n \rangle| < n_{\rm rms}/10$, is plotted as a function of $n_{\rm imp}$. We see that as $n_{\rm imp}$ decreases A_0 increases, reaching more than 1/3 at the lowest impurity densities. The fraction of area over which $|n(\mathbf{r}) - \langle n \rangle|$ is less than 1/5 of $n_{\rm rms}$ surpasses 50% for $n_{\rm imp} \lesssim 10^{10}$ cm^{-2}. Thus, much of the 2D landscape in this situation has very low ($\ll n_{\rm imp}$) carrier density with a few random electron-hole puddles. In Fig. 2(d), the dependence of the excess charge $\delta Q \equiv n_{\rm rms} \pi \xi^2$ on $n_{\rm imp}$ is shown. At high impurity densities ($\gtrsim 10^{12}$ cm^{-2}) and values of $d \gtrsim 1$ nm, δQ can be approximately identified with the average number of carriers per puddle; however, the above discussion and the results for A_0 allow us to recognize that δQ, for small $n_{\rm imp}$, *is not* the typical number of carriers per puddle. The reason is that for small $n_{\rm imp}$ (and/or d), because of the large fraction of area over which is $|n(\mathbf{r}) - \langle n \rangle| \ll n_{\rm rms}$, $n_{\rm rms}$ is much smaller than the typical carrier density in an electron-hole puddle of size ξ. At low $n_{\rm imp}$, δQ grossly underestimates the number of carriers in a typical puddle of size ξ.

We are now in a position to discuss the validity of our TF approach. The use of the TF theory is justified when the condition $|\nabla n(\mathbf{r})|/[n(\mathbf{r}) k_F(\mathbf{r})] \ll 1$ is satisfied. If we estimate $|\nabla n(\mathbf{r})| \approx n_{\rm rms}/\xi$, the above inequality implies $\sqrt{\pi n_{\rm rms}}\,\xi \gg 1$, i.e., $\delta Q \gg 1$. However, for small $n_{\rm imp}$ and d, $n_{\rm rms}$ greatly underestimates $|n|$ in the regions where it is inhomogeneous, i.e., in the electron-hole puddles of size ξ. We find that, at low $n_{\rm imp}$, $|n|$ in these electron-hole puddles is a factor of 10 or more higher than $n_{\rm rms}$. This can already be seen for relatively high values of $n_{\rm imp}$ and d: From Fig. 1(a), we see that $|n|$ inside the electron-hole puddles takes values as high as 8×10^{12} cm^{-2} whereas the corresponding value of $n_{\rm rms}$ is only 8×10^{11} cm^{-2} [Fig. 2(a)]. Even in the limiting case of an isolated impurity with $d = 0$, the density profile obtained using the TF approach [17] is very similar to the one obtained starting from the Dirac equation and treating the interaction via the renormalization-group method [18]. The additional $\delta(\mathbf{r})$ for $n(\mathbf{r})$ found in Ref. [18] (and [19]) in real graphene, in which the MDF model applies only at low energies, is regularized by $\max[d, a_0]$ [20]. Our results are therefore quantitatively accurate.

From the theoretical analysis [5,9–11] of experimental transport results [3], one obtains, for typical graphene samples on SiO_2, $d = 1$ nm and $n \approx 3 \times 10^{11}$ cm^{-2}. For these values, from Figs. 2(a) and 2(b), we see that $n_{\rm rms} = 3 \times 10^{11}$ cm^{-2} and $\xi = 9$ nm. The value of $n_{\rm rms}$ is in very good agreement with the recent STM [7] and single electron transistor (SET) [6] results. The value of ξ is also in very good agreement with the STM results and consistent with the results of Ref. [6] that, given the lower SET spatial resolution ($\gtrsim 150$ nm), could only provide for ξ an upper bound of 30 nm.

At a finite gate voltage V_g, the average carrier density $\langle n \rangle = C_g V_g / e$ is induced, where C_g is the gate capacitance. In our calculations we indirectly fix $\langle n \rangle$ by varying the chemical potential μ. The relation between μ and $\langle n \rangle$ is shown in Fig. 3(a). Contrary to ordinary parabolic-band fermionic systems, the relation between μ and $\langle n \rangle$ strongly depends on disorder even when exchange is neglected. This is also shown in Fig. 3(b) in which μ is plotted as a function of $n_{\rm imp}$ for a fixed value of $\langle n \rangle$. The dependence of $\mu(\langle n \rangle)$ on $n_{\rm imp}$ even without exchange is due to the fact that in graphene the kinetic energy does not scale linearly with n. From Fig. 3(a), we see that only for $n_{\rm imp} \lesssim 10^{10}$ cm^{-2} $\mu(\langle n \rangle)$ follows the equation valid for clean graphene. We

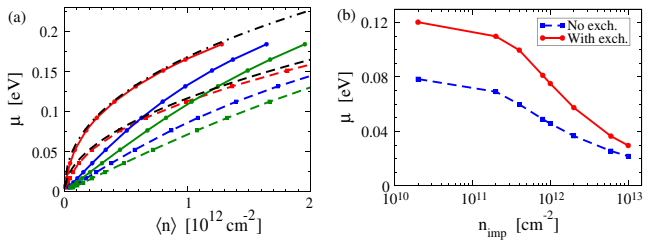

FIG. 3 (color online). Solid (dashed) lines: Results with (without) exchange. $\epsilon = 2.5$. (a) μ vs $\langle n \rangle$ for $n_{\rm imp} = 2 \times 10^{10}$ cm^{-2}, red lines; $n_{\rm imp} = 10^{12}$ cm^{-2}, blue lines; $n_{\rm imp} = 2 \times 10^{12}$ cm^{-2}, green lines. The black dotted-dashed (dashed) line shows $\mu(n)$ for clean graphene with (without) exchange. (b) μ vs $n_{\rm imp}$ for $\langle n \rangle = 5 \times 10^{11}$ cm^{-2}.

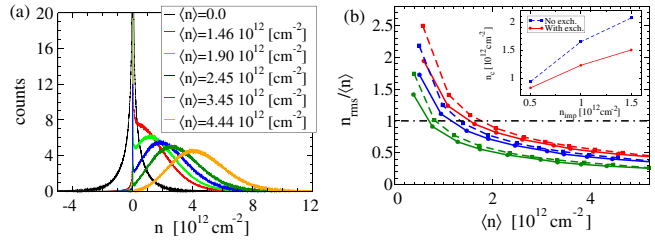

FIG. 4 (color online). Results away from the Dirac point assuming a SiO_2 substrate. (a) Density distribution averaged over disorder for different values of V_g for $d = 1$ nm and $n_{\rm imp} = 10^{12}$ cm^{-2}. (b) $n_{\rm rms}/\langle n\rangle$ vs $\langle n\rangle$ for $d = 1$ nm and: $n_{\rm imp} = 1.5 \times 10^{12}$ cm^{-2}, red lines; $n_{\rm imp} = 10^{12}$ cm^{-2}, blue lines; $n_{\rm imp} = 5 \times 10^{11}$ cm^{-2}, green lines. Inset: n_c vs $n_{\rm imp}$ for $d = 1$ nm. Solid (dashed) lines: Results with (without) exchange.

also notice that $\mu(\langle n\rangle)$ is strongly affected by exchange. The results of Fig. 3 demonstrate the interplay of disorder and interaction in graphene and show how the dependence of μ on $\langle n\rangle$, and, in particular, the average compressibility $1/(n^2 \partial\mu/\partial n)$, can be used to probe the strength of disorder and many-body effects. In Fig. 4(a), the disorder-averaged density distribution obtained including exchange is plotted for different values of $\langle n\rangle$, i.e., of V_g. For $V_g = 0$ the distribution has a strong peak [$\approx$20 times the maximum of the y scale of Fig. 4(a)] at $n = 0$. As V_g increases, the $n = 0$ peak survives, and a broad peak at finite n develops. For large enough V_g, the $n = 0$ peak disappears, and the density distribution is characterized only by the broad peak centered at $n = \langle n\rangle$. The results without exchange are qualitatively similar. The double peak structure for finite V_g provides direct evidence for the existence of puddles over a finite voltage range. High values of V_g remove one kind of puddles and increase the amplitude of the density fluctuations reflected in an increase of $n_{\rm rms}$. On the other hand, the ratio $n_{\rm rms}/\langle n\rangle$ decreases monotonically as a function of $\langle n\rangle$ as can be seen in Fig. 4(b). We can define a characteristic density n_c as the value of $\langle n\rangle$ for which $n_{\rm rms} = \langle n\rangle$ with $\Delta V_g = e n_c/C_g$ loosely measuring the width in gate voltage over which the transport properties of graphene are dominated by the density fluctuations around the Dirac point. The inset in Fig. 4(b) shows n_c as a function of $n_{\rm imp}$ for $d = 1$ nm. We can see that in current samples $n_{\rm rms} \gtrsim \langle n\rangle$ for carrier densities as high as $\langle n\rangle \approx 10^{12}$ cm^{-2}. The particular dependence of the carrier density distribution and $n_{\rm rms}$ on V_g is unique to inhomogeneities created by charged impurities and is a prediction that should be easy to verify experimentally.

We conclude by summarizing our key qualitative findings: (i) Both disorder and many-body effects become quantitatively very important on the chemical potential close to the Dirac point; (ii) many-body effects are more important at lower values of $n_{\rm imp}$; (iii) for low $n_{\rm imp}$, the ground state near the Dirac point is characterized by small puddles and large regions of almost zero ($|n| \ll n_{\rm imp}$) carrier density; (iv) in current samples $n_{\rm rms} \gtrsim \langle n\rangle$ for carrier densities as high as $\langle n\rangle \approx 10^{12}$ cm^{-2}; (v) the number of carriers per puddle is $\sim$1–5 at low carrier densities; (vi) our theory agrees well with the existing data [6,7] but more experiments will be required to test our quantitative predictions.

We thank S. Adam, M. Fuhrer, E. H. Hwang, and especially A. H. MacDonald for discussions. The numerical calculations have been performed on the University of Maryland High Performance Computing Cluster (HPCC). This work is supported by NSF-NRI-SWAN and U.S.-ONR

[1] K. S. Novoselov *et al.*, Science **306**, 666 (2004).
[2] E. Fradkin, Phys. Rev. B **33**, 3257 (1986); A. W. Ludwig *et al.*, Phys. Rev. B **50**, 7526 (1994); I. L. Aleiner and K. B. Efetov, Phys. Rev. Lett. **97**, 236801 (2006); A. Atland, Phys. Rev. Lett. **97**, 236802 (2006); N. M. R. Peres *et al.*, Phys. Rev. B **73**, 125411 (2006); L. Fritz *et al.*, Phys. Rev. B **78**, 085416 (2008); A. Kashuba, Phys. Rev. B **78**, 085415 (2008); J. H. Bardarson *et al.*, Phys. Rev. Lett. **99**, 106801 (2007); K. Nomura *et al.*, Phys. Rev. Lett. **99**, 146806 (2007).
[3] Y.-W. Tan *et al.*, Phys. Rev. Lett. **99**, 246803 (2007); J. H. Chen *et al.*, Nature Phys. **4**, 377 (2008).
[4] M. .I. Katsnelson *et al.* Nature Phys. **2**, 620 (2006).
[5] E. H. Hwang *et al.* Phys. Rev. Lett. **98**, 186806 (2007).
[6] J. Martin *et al.*, Nature Phys. **4**, 144 (2008).
[7] V. W. Brar *et al.*, Bull. Am. Phys. Soc. **53**, U29.00003 (2008); V. W. Brar *et al.*, Appl. Phys. Lett. **91**, 122102 (2007).
[8] A. H. Castro Neto and E. A. Kim, arXiv:cond-mat/0702562v2; Fernando de Juan *et al.*, Phys. Rev. B **76**, 165409 (2007); L. Brey and J. J. Palacios, Phys. Rev. B **77**, 041403(R) (2008); F. Guinea *et al.*, Phys. Rev. B **77**, 075422 (2008).
[9] K. Nomura and A. H. MacDonald, Phys. Rev. Lett. **96**, 256602 (2006).
[10] S. Adam *et al.*, Proc. Natl. Acad. Sci. U.S.A. **104**, 18 392 (2007).
[11] T. Ando, J. Phys. Soc. Jpn. **75**, 074716 (2006).
[12] Y. Barlas *et al.*, Phys. Rev. Lett. **98**, 236601 (2007).
[13] E. H. Hwang *et al.*, Phys. Rev. Lett. **99**, 226801 (2007); E. G. Mishchenko, Phys. Rev. Lett. **98**, 216801 (2007);
[14] K. I. Bolotin *et al.*, Solid State Commun. **146**, 351 (2008); Xu Du *et al.*, arXiv:0802.2933v1; S. Adam and S. Das Sarma, Solid State Commun. **146**, 356 (2008).
[15] M. Polini *et al.*, Phys. Rev. B **78**, 115426 (2008).
[16] B. I. Shklovskii, Phys. Rev. B **76**, 233411 (2007).
[17] M. I. Katsnelson, Phys. Rev. B **74**, 201401(R) (2006).
[18] R. R. Biswas *et al.*, Phys. Rev. B **76**, 205122 (2007).
[19] A. V. Shytov *et al.*, Phys. Rev. Lett. **99**, 236801 (2007); I. S. Terekhov *et al.*, Phys. Rev. Lett. **100**, 076803 (2008).
[20] M. M. Fogler *et al.*, Phys. Rev. B **76**, 233402 (2007); D. D. Novikov, Phys. Rev. B **76**, 245435 (2007); V. M. Pereira *et al.*, Phys. Rev. Lett. **99**, 166802 (2007).